

Septa

M. Paraliev

Paul Scherrer Institute, Villigen PSI, Switzerland

Abstract

In the Septa I and Septa II lectures we introduce the basic concept of particle accelerator septa devices—key elements of beam injection and extraction systems. The basics of charged particle beam electrostatic and magnetic deflection are presented and a comparison between the two schemes is given. Different septa types and their specifics are described and most are illustrated with real septa designs from accelerator laboratories around the world. Design examples are used to emphasize the important septa parameters and their limitations. Finally, the presented equations for electrostatic and magnetic deflection are mathematically derived.

Keywords

Electrostatic septum; septum magnet; injection; extraction.

1 Introduction

For efficient beam switching, injection, or extraction a special type of beam deflecting device is needed. Such devices are characterized by two distinctive deflecting regions in order to switch, merge, or separate charged particles beams. Typically one region provides (ideally) zero deflection and the other—a significant constant deflection. However, there are designs where both regions provide deflection but in opposite directions. The main objective of the device is to ensure an abrupt deflecting field change between the two regions, with a separating barrier (septum) that is as thin as possible and a minimum leakage field.

The article gives an overview of the conventional septa deflecting schemes and designs. It uses example hardware implementations to discuss some specific design features of the septa.

The essential mathematical expressions that describe electrostatic and magnetic deflections are presented. All quantities are in SI units unless other is stated.

2 Septum

The term *septum* (plural *septa*) means ‘a partition’, ‘a wall’, ‘a barrier’ that separates two cavities or two chambers. It is used in different science and technology fields such as biology, mechanics, particle physics, etc. The word has a Latin origin and it is a derivate of the word *saepio* (*sēpiō*) meaning ‘to surround’, ‘to enclose’, ‘to fence in’ something. In particle accelerators, a septum divides two distinctive field regions in order to selectively deflect charged particle beams to one or other side of it. Often the device that embodies the septum is called a ‘septum’ as well (e.g., electrostatic septum, septum magnet, etc.). Septa, often accompanied by kicker devices, are an essential part of charged particle beam injection and extraction systems.

2.1 Basic concept and terminology

A magnetic septum has a lot in common with dipole (bending) magnets but it is more complex due to the necessity of having an abrupt field change. Figure 1 shows schematically the general layout and basic parameters of a septum. The *bending angle* θ (usually in radians or milliradians) is one of the most

important parameters of a septum. It expresses how much the trajectory of the deflected charged particle beam (hereafter referred to by only ‘*beam*’) diverges from the straight trajectory. The bending angle depends on particle type (rest mass and charge), particle momentum (kinetic energy), deflecting field (type, strength, and direction), and effective length of the septum. *Bending radius* R (usually in metres) is another way of expressing the deflection of the *beam*. *Sagitta*, s (usually in metres or millimetres), gives the largest distance between the arch of the *beam* trajectory and its chord. Together with the *deflecting gap width*, w (usually in metres or millimetres), it is an important parameter for designing a septum large enough to accommodate fully the bent beam, especially if the deflecting gap does not follow the *beam* trajectory. *Septum thickness*, t (usually in millimetres), describes the distance between the aperture walls of the straight and the deflected *beam*. Septum thickness is one of the important parameters of the device and it is often a delicate engineering compromise to meet the controversial mechanical, thermal, electrical, and leakage field requirements of the septum. A thin septum is always an advantage, whether it is for slow (scraping) extraction or for fast (e.g., kicker based) extraction. In the first case, a thin septum reduces *beam* losses and radiation loading. In the second, it reduces the required spatial separation of the two *beams*, relaxing the requirements of the kicker. *Septum length*, l (usually in metres), gives the distance the *beam* travels under the deflecting field. In practice, the length of the field region is different from the mechanical length of the device due to the mechanical construction and fringe fields at the septum entrance and exit. An integral equivalent value, called the *effective length*, is used to describe the proper *beam*–field interaction distance.

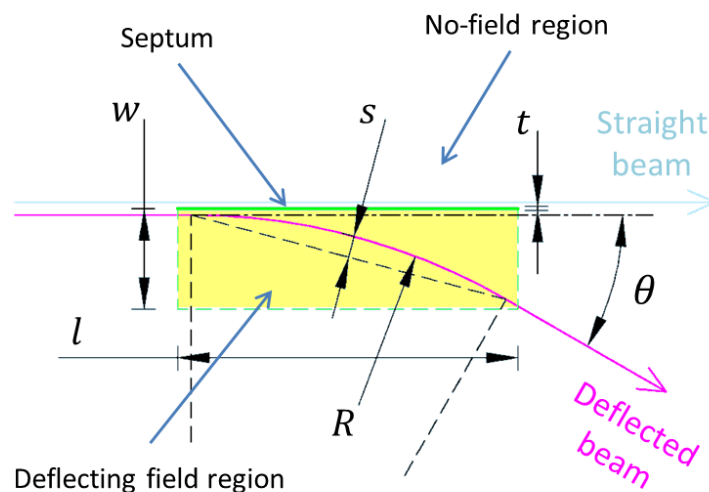


Fig. 1: Schematic representation of a septum

2.2 Key objectives

The key objectives to a septum may be summarized as follows.

- (i) *Good field region* – The bending field region should provide an adequate deflecting field (type, strength, and direction) in order to achieve the required *beam* deflection. The field should be constant (homogeneous) not to affect the *beam* optics (although there are some exceptions when the septum has an optics functionality too).
- (ii) *Field free region* – In order not to disturb the trajectory of the ‘straight’ beam, the ‘field free region’ (or ‘zero field region’) should have very low residual deflecting field. This is of key importance for circulating *beam* accelerators, where the unwanted trajectory disturbance can accumulate (depending on the machine tune) each time the *beam* passes through the septum.

- (iii) *Accommodate the beam* – The aperture of the device should be large enough to accommodate the straight and the bent *beams* taking in account *beam* trajectory and *beam* size (depending on *beam* emittance and the particular beta function at the location of the septum)
- (iv) *Beam impedance* – Irregularities in the *beam* chamber introduce variation of the electrical impedance seen by the *beam*. This can create unwanted electric resonances that are excited by the passing *beam*. Especially in circular accelerators these resonances can lead to *beam* instabilities.
- (v) *Vacuum* – Vacuum quality is an important parameter for the particle accelerators. When designing septa, care should be taken to avoid materials that are not compatible with a vacuum (emitting or having a large capacity to absorb gases, sublimating etc.) If a high vacuum is required, the design should be bake-out compatible and it should provide enough vacuum ‘conductance’ to the corresponding vacuum pumps. If vacuum conductance cannot be further improved, a number of special measures can be taken (such as non-evaporable getter (NEG) coating etc.) to reduce locally the background gas pressure.
- (vi) *Positioning and mechanical stability* – The correct position of the septum with respect to the *beam* is crucial for its proper and efficient operation. High resolution, remotely controlled mechanical actuators are often used to position septa. Proper mechanical support should be provided to bear the electromagnetic forces. Delicate septa (thin foils or wires) should be attached using special tensioners to cope with the thermal deformation. In pulsed devices, mechanical absorbers may be necessary to limit mechanical shockwave propagation.
- (vii) *Synchrotron radiation* – If the charged particle *beam* is deflected it emits electromagnetic waves (synchrotron radiation). This process might affect the properties of the *beam* or it could interact with the vacuum chamber or other devices. Since synchrotron radiation power depends strongly on the deflecting angle, usually it does not have a significant effect in small deflection angle septa.
- (viii) *Radiation effects* – Septa are often the most irradiated components of a particle accelerator. In some cases, the excessive radiation can cause material degradation especially for some electrical insulators. Sensitive electronic components could be affected as well if placed in proximity to the septa. Proper shielding should be used to ensure personnel radiation safety outside of the accelerator tunnel during operation. Material activation is another problem that should be taken in account. After being in operation, the septa could be activated and could remain radioactive for extensive periods of time after they are out of service. Remaining radioactive emission could make septa very difficult to service and handle due to the radiation hazards.
- (ix) *Thermal management* – Proper thermal management of the septa is crucial for their reliable operation. Excessive heat load could be generated by *beam* irradiation and/or by flowing electrical currents (in electromagnetic septa). Proper cooling should be provided to keep the septa temperature within safe limits.
- (x) *Machine and personal protection* – Often septa must meet very demanding requirements and their operating point could be very close to the material damage threshold. In these cases, a proper machine protection system should be provided to prevent damage in case of system failure (fault in power supply, cooling system etc.) or operator error (*beam* miss-steering, incorrect operation conditions etc.). Septa themselves could be part of the machine or personnel protection system, for example disabling the injection in a circular accelerator. The risks associated with high energy densities and radiation effects in septa and the associated equipment should be carefully evaluated and proper measures should be taken to protect the personnel.
- (xi) *Reliability/Serviceability/Reparability* – The complexity and the demanding requirements that septa should meet make them prone to failures. Constructors should carefully assess the reliability of the device as well as the procedures for maintenance and repair. Proper safety measures should

be taken to handle and recycle activated components. Depending on the estimated mean time between failure, expected device lifetime, facility importance, and projected facility life span, the adequate number of reserve devices can be foreseen. Resources should be planned for the necessary long-term maintenance.

- (xii) *Building costs versus operation costs* – As in any engineering process, care should be taken to optimize construction costs against running costs. Often assessing the running costs is not a straightforward task. Besides the obvious costs for electricity, there are ‘hidden’ costs such as: for running and maintaining the supporting systems (cooling, controls etc.), consumables (e.g., in cases of high radiation environment, insulating oil, and cables), maintaining qualified supporting personnel, and so on. Proper assessment of the running costs may influence strongly the device design.

(This list is not exhaustive.)

3 Types of septa

Typically, charged particle beams are deflected using electric and/or magnetic fields. However, there are other, more ‘exotic’ methods to deflect *beams* as well (such as using bent crystals, see Refs. [1–2] etc.) but these are beyond the scope of this overview.

The force \vec{F} exerted on a point charge by electromagnetic fields is given by Eq. (1), which is named after the prominent Dutch physicist Hendrik Lorentz. Some historians suggest that the formula derivation has an even earlier origin and attribute it to Oliver Heaviside or James Maxwell.

$$\vec{F} = q\vec{E} + q\vec{v}\times\vec{B}, \quad (1)$$

where q is the electric charge of the particle, \vec{E} is the electric field, \vec{v} is the instantaneous velocity of the particle, and \vec{B} is the magnetic flux density. The first term on the right-hand side of Eq. (1) accounts for the electric field interaction. The exerted electric force depends only on the strength of the electric field and particle charge. The second term accounts for the magnetic interaction, and the force depends on the magnetic field strength as well as on the particle’s charge and instantaneous velocity

In accelerators, charged particles often travel with relativistic speeds and the relativistic effects have to be taken in account when dealing with their dynamics.

3.1 Electrostatic deflection

The first option for deflecting *beams* is to use an electric field (electrostatic deflection, also called electric deflection). The force exerted on the particle \vec{F}_E is given by Eq. (2) and it is in the direction shown in Fig. 2.

$$\vec{F}_E = q\vec{E}, \quad (2)$$

where q is the electric charge of the particle and \vec{E} is the electric field. The deflecting force is collinear with the electric field. Positive charges are deflected in the direction of the electric field lines, negative charges are deflected in the opposite direction.

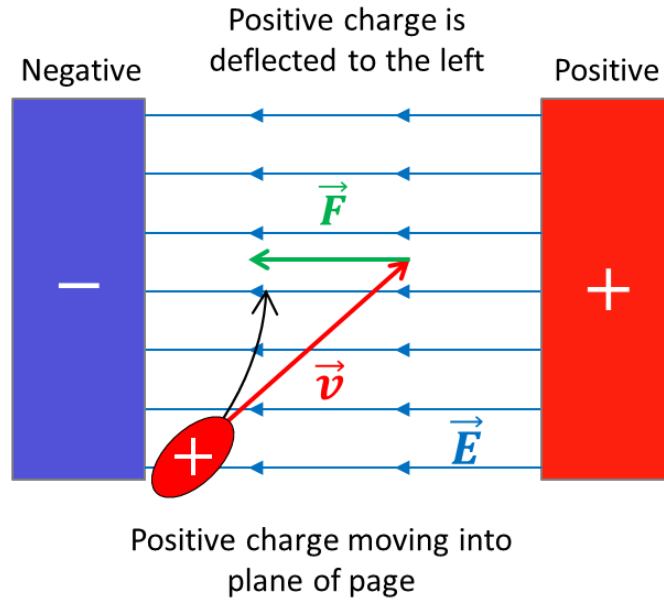


Fig. 2: Electric deflection

Conventions:

- Force on a *positive* point charge.
- Electric field lines go from the *positive* electrode to the *negative* one.
- Opposite electric charges attract each other and *like* electric charges repel.

Equation (3) expresses the bending angle θ_E of a particle with elementary charge, where E is the electric field, l_{eff} is the effective length of the device, β is a dimensionless relativistic coefficient that gives the fraction of the speed of light at which the particles travel, p is the *beam* momentum in gigaelectronvolts over the speed of light (GeV/c), U is the deflecting voltage and d is the distance between the deflecting electrodes, see Refs. [3,4].

$$\theta_E \approx \frac{E \cdot l_{\text{eff}}}{10^9 \cdot \beta \cdot p} = \frac{U \cdot l_{\text{eff}}}{10^9 \cdot \beta \cdot p \cdot d} \tag{3}$$

Equation (3) uses *the small angle approximation* ($\tan(\theta) \approx \theta$) which is valid for angles up to ~ 0.17 rad ($\sim 10^\circ$) with an error below 1%. Attention should be paid to use of the correct measurement units (especially for *beam* momentum).

Note:

- Momentum units conversion $p \left[\frac{\text{kg}\cdot\text{m}}{\text{s}} \right] = \frac{q_e}{c} p \left[\frac{\text{eV}}{c} \right]$.

Derivation of the electric deflection equation is included in Appendix A.

3.2 Magnetic deflection

The second option for deflecting *beams* is to use a magnetic field (magnetic deflection). The force exerted on the particle \vec{F}_M is given by Eq. (4) and it is in the direction shown in Fig. 3.

$$\vec{F}_M = q\vec{v} \times \vec{B}, \quad (4)$$

where q is the electric charge of the particle, \vec{v} is the instantaneous velocity of the particle, and \vec{B} is the magnetic flux density. The deflecting force is a cross product of \vec{v} and \vec{B} and it is perpendicular to the propagation direction and magnetic field. Positive charges are deflected in the direction defined by the *right-hand rule*; negative charges are deflected in the opposite direction.

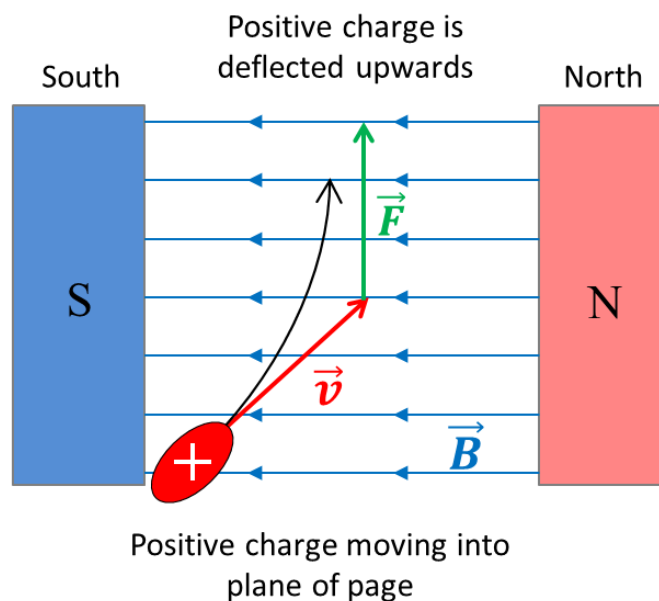


Fig. 3: Magnetic deflection

Conventions:

- Force on a **positive** point charge.
- Magnetic **field** lines go from the **North pole** to the **South pole** of the magnet (in the space outside the magnet).
- **Right-hand rule**: If the thumb points in the direction of motion and the index finger points in the direction of the magnetic field, the magnetic force goes in the direction of the middle finger.

Equation (5) expresses the bending angle θ_M of a particle with elementary charge, where B is the magnetic flux density, l_{eff} is the effective length of the device, p is the *beam* momentum in giga-electronvolts over the speed of light (GeV/c), n is the number of turns of the magnet winding, I is the deflecting current, and d is the distance between the magnetic poles, see Refs. [3–6].

$$\theta_M \approx \frac{0.3 \cdot B \cdot l_{\text{eff}}}{p} \approx \frac{3.76 \cdot n \cdot I \cdot l_{\text{eff}}}{10^7 \cdot p \cdot d}. \quad (5)$$

Equation (5) uses *the small angle approximation* ($\tan(\theta) \approx \theta$) which is valid for angles up to ~ 0.17 rad ($\sim 10^\circ$) with an error below 1%. Attention should be paid to use of the correct measurement units (especially for *beam* momentum).

Note:

- Magnetic flux density approximation $B \approx \frac{\mu_0 n I}{d}$.
- Momentum unit conversion $p \left[\frac{\text{kg}\cdot\text{m}}{\text{s}} \right] = \frac{q_e}{c} p \left[\frac{\text{eV}}{c} \right]$.

Derivation of the magnetic deflection equation is included in Appendix B.

3.3 Electrostatic versus magnetic deflection

The duality of *electromagnetism* suggests that the two deflection methods should be somehow equivalent. Let's compare the deflection capability of an electric and magnetic field with the same energetic characteristics. Equations (6) and (7) give the energy density, W_E and W_M , of an electric and magnetic field in free space, see Ref. [7]:

$$W_E = \frac{\epsilon_0 E^2}{2}, \quad (6)$$

$$W_M = \frac{B^2}{2\mu_0}, \quad (7)$$

where ϵ_0 is the permittivity of free space, E is the electric field, B is the magnetic flux density, and μ_0 is the permeability of free space. The relation between an electric and magnetic field with the same energy density could be found by equating Eqs. (6) and (7):

$$E = \frac{1}{\sqrt{\mu_0 \epsilon_0}} B \quad \text{or} \quad E = cB, \quad (8)$$

where c is the speed of light in free space. Using the scalar form of Eqs. (2) and (4), we can see that electric deflecting force F_E and magnetic force F_M for fields with the same energy density depends only on the charged particle instantaneous velocity v and it is *the same for relativistic particles* ($v = c$).

$$F_E = qE = qcB, \quad (9)$$

$$F_M = qvB. \quad (10)$$

Note:

- Speed of light in free space is equal to 299 792 458 m/s *exactly!*
- On the other hand, μ_0 and ϵ_0 are *irrational numbers*.

Since most particle accelerators deal with relativistic *beams* and since, practically, producing a magnetic field is *much easier* than producing an electric one with the same energy density, the majority of accelerator' deflecting devices are magnetic. Equation (11) expresses the equivalence of electric and magnetic field deflection, where the electric field E is in gigavolts per metre (GV/m), B is the magnetic flux density, and β is the dimensionless relativistic coefficient that gives the fraction of the speed of light at which the particles travel.

$$\frac{3.3}{\beta} E = B. \quad (11)$$

Table 1 compares the deflecting capability of an electric and magnetic field for electrons and protons with different momenta. An electric field of 10 MV/m is taken as a comparison benchmark since it is widely accepted as the practical maximum electric field limit.

Table 1: Electric and magnetic deflection for different particle momenta

β	γ	$p_{\text{electrons}}$ (MeV/c)	p_{protons} (GeV/c)	Electric field (MV/m)	Equivalent magnetic field (T)	
0.001	1.000	0.0005	0.0009	10.00	33.356	Non-relativistic
0.01	1.000	0.0051	0.0094	10.00	3.336	
0.1	1.005	0.0514	0.0944	10.00	0.334	
0.3	1.048	0.1607	0.2955	10.00	0.111	
0.5	1.155	0.2950	0.5425	10.00	0.067	
0.9	2.294	1.0552	1.9401	10.00	0.037	Relativistic
0.99	7.089	3.5864	6.5944	10.00	0.034	
0.999	22.366	11.4185	20.9955	10.00	0.033	
0.9999	70.712	36.1328	66.4386	10.00	0.033	
0.99999	223.607	114.2698	210.1114	10.00	0.033	
0.999999	707.107	361.3552	664.4349	10.00	0.033	

Electric field deflection has an advantage for low β beams (low energy, heavy particles) as well as in some special cases when there are geometrical advantages. Table 2 summarizes the basic pros and cons of the two septa types.

Table 2: Advantages and disadvantages of electrostatic and magnetic septa

Electrostatic septum	Magnetic septum
+ Nearly perfect ‘zero-field’ region	+ Strong deflection
+ Thin septum	+ More effective for relativistic beams
+ Low mass density (low beam interaction)	+ In-vacuum and in-air design is possible
+ Better for non-relativistic beams	– Thick septum
– Difficult to have high fields	– Field leakage
– Less effective for relativistic beams	– Non-uniform field region
– High voltages handling	– Interaction with other magnets
– Strictly in-vacuum design	– High currents handling

4 Electrostatic septum

As illustrated schematically in Fig. 4, an electric field is established between a high voltage (HV) electrode and a septum foil. The injected or extracted *beam* passes through the electric field region and is deflected. Using electrostatic screening (*Faraday cage effect*) a zero-field region is created for the (circulating) *beam* that goes straight. Due to the practically perfect electric field screening from even very thin conductor foils, the straight *beam* passes undisturbed. Due to the high electric fields electrostatic septa designs are exclusively ‘in-vacuum’.

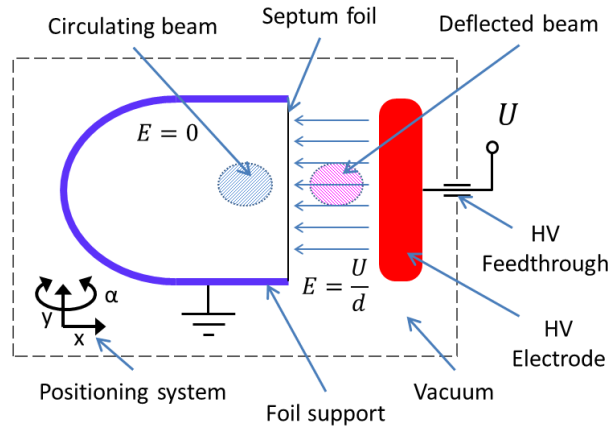


Fig. 4: Schematic view of electrostatic septum

A thin foil or wire array is used to minimize the interaction with the *beam* (reduces *beam* losses and radiation levels). To align the septum with the *beam*, often the septum and its support are attached to a remotely controlled, precision positioning system. Since the zero-field region is a relatively confined volume, some holes away from the HV electrode are necessary to ensure good vacuum conductivity and to maintain a low background gas pressure.

4.1 Foil septum

Foil septa benefit from the very thin septum conductor (the foil) used to separate the field and zero-field region. Due to its small cross-section the foil (foil thickness down to 100 μm) interacts less with the *beam* and reduces losses and radiation. Figure 5 shows an example of a foil septum, ‘Septum 23’, used in the proton synchrotron ring at CERN for resonant slow extraction (see Refs. [8–9]). Table 3 summarizes its technical parameters.

Table 3: Technical specification of ‘Septum 23’

Parameter	Value
Electrode length, mm	778
Gap width, mm	17
Beam momentum, GeV/c	24
Deflection angle, mrad	0.28
Septum thickness, μm	100
Vacuum pressure, mbar	10^{-9}
Voltage, kV	260
Electric field, MV/m	up to 15
Septum foil material	Molybdenum
Electrode material	Anodized Peraluman 300
In situ bake-able	Yes

‘Septum 23’ (Fig. 5) uses polished 100 μm molybdenum foil (as septum) and an anodized aluminium alloy HV electrode that enables an electric field up to 15 MV/m after conditioning. Polished stainless steel deflectors confine the electric field and help to extend the ‘good field’ region to 40 mm. They also protect HV active parts from titanium deposition (from sublimation vacuum pumps). The septum is equipped with an in-vacuum infrared lamp in order to allow in situ bake-out. The foil is

attached using tensioners that reduce the mechanical stress in the foil due to different thermal loadings in different operating modes (bake-out or *beam* thermal loading), see Ref. [8]. A series of holes in the foil support provide good vacuum conductivity between the ‘zero-field’ region and the rest of the chamber. The septum and the HV electrode are equipped with a precise positioning system (translation resolution 100 μm) in order to align well with the *beam*. The septum can also be moved away from the *beam* in case it is not used to minimize *beam* losses. Due to radiation degradation effects, the insulating oil in the HV feedthroughs is regularly changed (every 3 months) and the close HV cables are replaced annually, see Ref. [9]. The maintenance of the septum is difficult because it is radioactively ‘activated’.

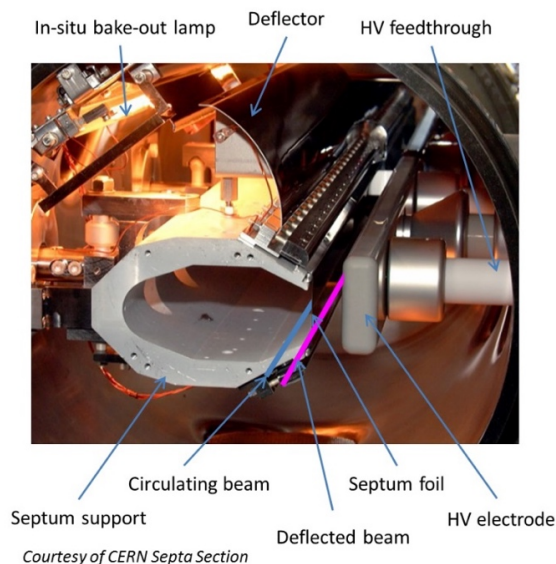


Fig. 5: ‘Septum 23’ proton synchrotron ring at CERN

4.2 Foil septum with inverted design

Another variation of the foil septum has a so-called ‘inverted’ design. In this case, the field is confined inside the foil holder, as shown in Fig. 6. This provides better control over the electric field distribution and enables one-sided mechanical support, leaving space for additional in-vacuum components in the ‘zero-field’ region, but makes the construction of the HV feedthrough more complex. A typical example (Fig. 6) is the injection electrostatic septum (ES) designed for the National Centre of Oncological Hadrontherapy (CNAO) in Italy, see Refs. [10,11]. Table 4 summarizes its technical data.

Table 4: Technical specification of injection SE for CNAO

Parameter	Value
Electrode length, mm	800
Gap width, mm	25
Beam momentum, MeV/c	20
Deflection angle, mrad	60
Septum thickness, μm	100
Vacuum pressure, mbar	10^{-9}
Voltage, kV	69
Electric field, MV/m	2.8
Septum foil material	Molybdenum
Electrode material	Stainless steel

This particular design comprises two straight sections to follow the trajectory of the deflected *beam*. The whole septum support is attached to a positioning system with ± 5 mm range.

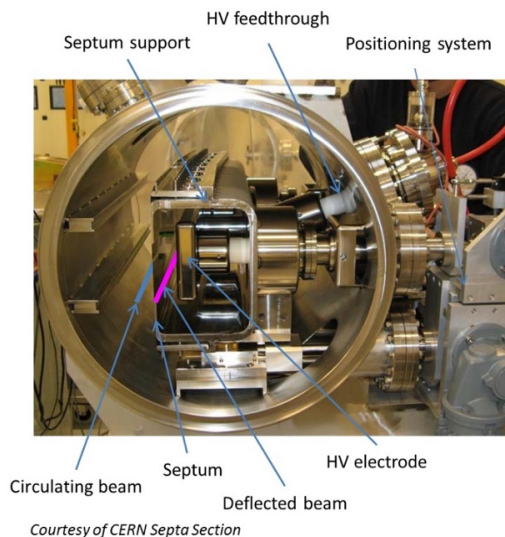


Fig. 6: Foil septum with ‘inverted’ design, CNAO injection ES

4.3 Diagonal foil septum

A diagonal foil electrostatic septum (ER.SEH10, Ref. [12]) is used in the low energy ion ring (LEIR) at CERN. It allows for a combined longitudinal and transverse injection scheme. The foil septum is tilted by 30° to provide the necessary diagonal electric field. The foil and the HV electrode are mechanically polished to improve their electrical breakdown performance. The septum–HV electrode system is conditioned to a higher than nominal voltage in order to ensure reliable operation. A carbon resistor is used to decouple the HV electrode from the supply cable to limit the discharge energy in case of breakdown between the HV electrode and septum.

Table 5: Specification of injection electrostatic septum ER.SEH10 for LEIR

Parameter	Value
Electrode length, mm	720
Gap width, mm	40
Beam momentum, MeV/nucleon	4.2
Deflection angle, mrad	28.9
Septum thickness, μm	100
Vacuum pressure, mbar	10^{-12}
Voltage, kV	51
Electric field, MV/m	1.12
Septum foil material	Molybdenum
Electrode material	Titanium

Special mechanical assembly is used to keep the septum foil in tension and to compensate for the different thermal expansions of the foil and the stainless steel support. Even after a 300°C bake-out, the

alignment of the foil remains within 100 μm . Both septum and cathode have independent alignment systems. Figure 7 shows the design of the septum.

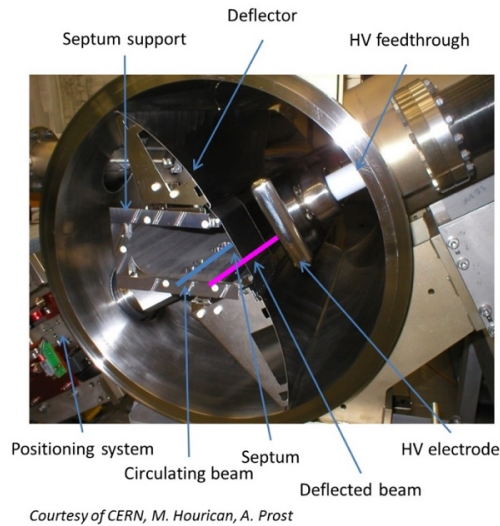


Fig. 7: Design of LEIR injection electrostatic septum ER.SEH10

4.4 Wire septum

In wire septa, the foil is replaced by an array of thin metallic wires. There are several advantages to using a wire array as a septum: Due to the gap between the wires the effective density of the septum is reduced. This leads to less interaction with the *beam* and lower *beam* losses and radiation. Often the wires have individual tensioners that in case of a failure take the broken wire away from the *beam*, keeping the septum operational. Wire septa allow better vacuum conductance for the zero-field region. There are some drawbacks associated with the wire septa as well. The wire array is not a continuous field barrier and allows some field penetration through the septum. This depends on the wire diameter d and wire spacing D . Let's define a wire density coefficient k as the ratio between the wire diameter d and the distance between the wires D . Figure 8 summarizes the results of 3D electrostatic simulation of the leakage field at a distance of $2 \times D$ for different values of the wire density coefficient k .

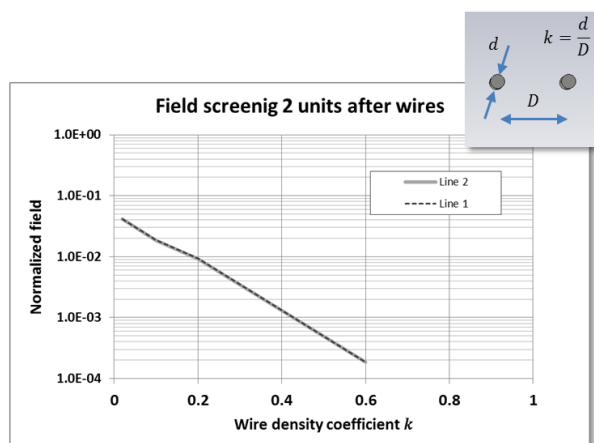


Fig. 8: Field penetration through wire septum at distance $2 \times D$ after the septum as a function of the wire density coefficient, k .

Even not very dense wire arrays ($k = 0.1$) provide ~ 53 times field reduction at a distance of $2 \times D$. Even though this field leakage is small it could move some ionized background gas molecules from the circulating *beam* (zero-field) area to the field gap. They will then be accelerated by the main septum field and they will be smashed into the HV electrode, increasing the chance of electrical breakdown. Special additional electrodes (ion traps) can be used to counter the leakage field and to clear the ions from the zero-field area of the septum.

A typical example of a wire septum is the ZS electrostatic septum in the super proton synchrotron (SPS) at CERN, allowing for both fast and slow extraction (see Ref. [13]). To obtain the required deflection, 5 identical wire septa are used. Table 6 gives the technical parameters of each of these septa and Fig. 9 shows their construction.

ZS septa are prone to electrical breakdown due to background gas ionization and they are fitted with upper and lower ion trap electrodes. A spark protection system (Ref. [14]) deactivates the devices if breakdowns are too frequently detected. The septa are equipped with a remote controlled mover system in order to be aligned with the *beam*. If not used, they can be completely retracted. Due to the different possible modes of operation, measures have to be taken to protect the ZS wire septum from *beam* induced overheating, caused by machine failure or operator error (Ref. [15]).

Table 6: Specification of the individual septa unit part of ZS electrostatic SPS extraction septum

Parameter	Value
Electrode length, mm	2997
Wire material	W74Re26
Wire diameter, μm	50 to 100
Wire spacing, mm	1.5
Gap width, mm	20
<i>Beam</i> momentum, GeV/c	450
Deflection angle, μrad	~ 70
Vacuum pressure, mbar	10^{-12}
Voltage, kV	220
Ion traps voltage, kV	3 to 6.5
Electric field, MV/m	up to 11
Electrode material	Anodized aluminium

There are even more challenging proposed electrostatic septum designs using extremely thin, low atomic number material wire arrays, curved under the force of an electric field, such as the mini-wire-septum proposed by H. Schönauer that can provide an additional collimation function (see Refs. [16,17]).

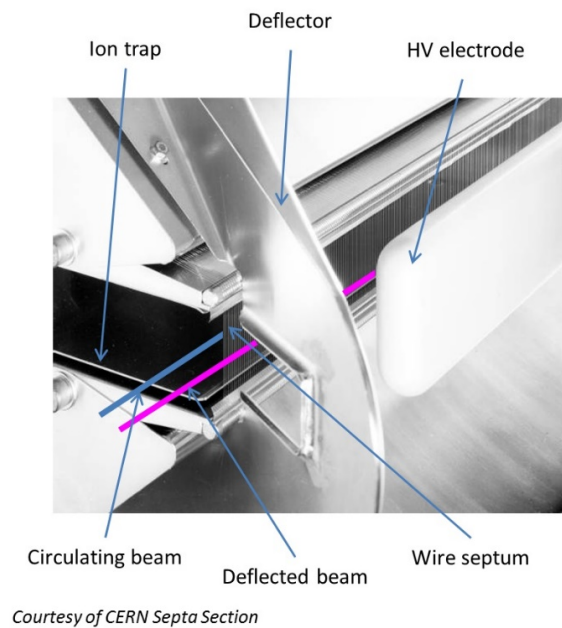


Fig. 9: Wire septum ZS, SPS, CERN

4.5 Practical considerations

- (i) *Very thin septa* – Small septa thicknesses (or diameter) require a stress relief mechanism (tensioners) to cope with the deformation due to thermal stress.
- (ii) *Low atomic number material* – Low atomic number septum materials are welcomed because they interact less with the *beam* and consequently generate less radiation.
- (iii) *High electric field* – Special surface treatment of the septum and HV electrode followed by conditioning should be considered to operate reliably at high electric field without breakdown.
- (iv) *Good field region* – Homogeneity of the field in the ‘good field’ region could be improved using a suitable gap geometry and deflectors.
- (v) *Field leakage compensation* – Wire septa may need leakage field compensation.
- (vi) *Beam impedance* – Measures should be taken to keep the *beam* impedance changes small, especially in circular accelerators, to avoid *beam* instabilities.
- (vii) *HV handling* – Mechanical components that serve as electrical isolators should have large enough creepage distances to avoid surface discharges. Triple points (metal–vacuum–isolator) should be carefully designed to cope with the enhanced electric field in these regions.
- (viii) *Insulators degradation* – Materials should be carefully chosen to withstand radiation. Organizational measures should be taken to regularly replace the vulnerable materials (oil, cables).
- (ix) *Alignment* – A proper positioning system should ensure good septum alignment.
- (x) *Good vacuum* – The design should meet the particular vacuum requirements, including bake-out capabilities.
- (xi) *Background gas ionization* – Measures should be taken to minimize the amount of ionized background gas molecules (good vacuum, ion traps) that could initiate a breakdown.
- (xii) *Machine protection* – Proper machine protection should be used to protect delicate septa.
- (xiii) *Activation* – Maintenance should be done according to the radiation safety regulations.

(This list is not exhaustive.)

5 Magnetic septum

In a typical magnetic septum, illustrated schematically in Fig. 10, the deflected *beam* goes through a homogeneous magnetic field that is established between two magnetic poles. The straight (circulating) *beam* passes next to main magnetic circuit ‘seeing’ as little as possible the magnetic field. Often magnetic screening techniques are used to shield the straight *beam* further.

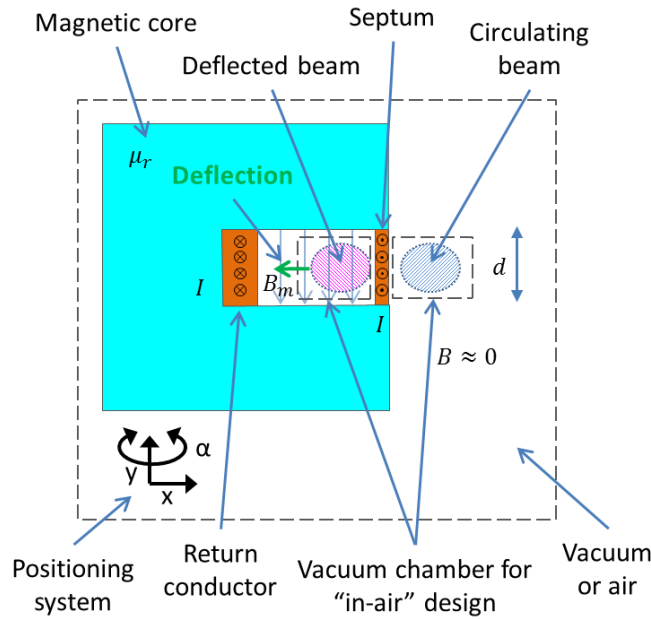


Fig. 10: Schematic view of magnetic septum

Magnetic septa are classified according to the magnetic field variation in time, as shown in Fig. 11. Essentially, they can have an ‘in-vacuum’ or ‘in-air’ design.

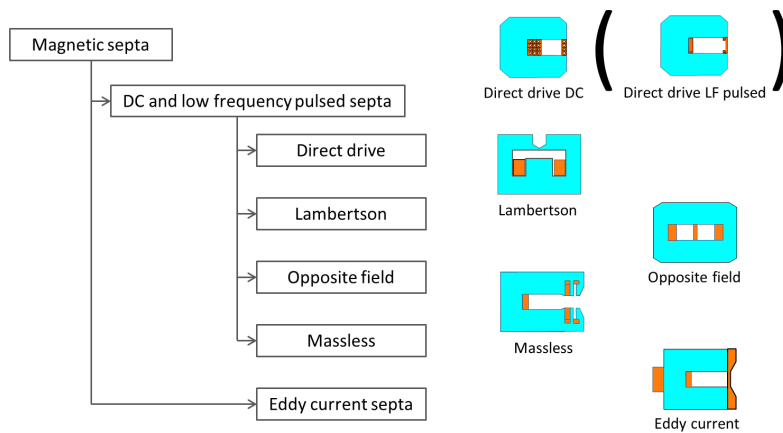


Fig. 11: Magnetic septa classification and schematic symbols

5.1 Direct drive DC septum

The direct drive DC septum (or ‘C’ type active septum magnet) is a type of window frame magnet with one of the legs removed. The septum is used as one of the magnet’s conductors and the return conductor is inside the magnetic core, see Ref. [18]. Field quality in the field region is good due to the magnet geometry. The septum is relatively thick in order to handle high currents. In circular machines the DC operation can push the acceptable leakage field limits further down because the circulating *beam* will be disturbed continuously each time it passes the septum. A static magnetic simulation example (Fig. 12) is used to illustrate the field distribution along line A.

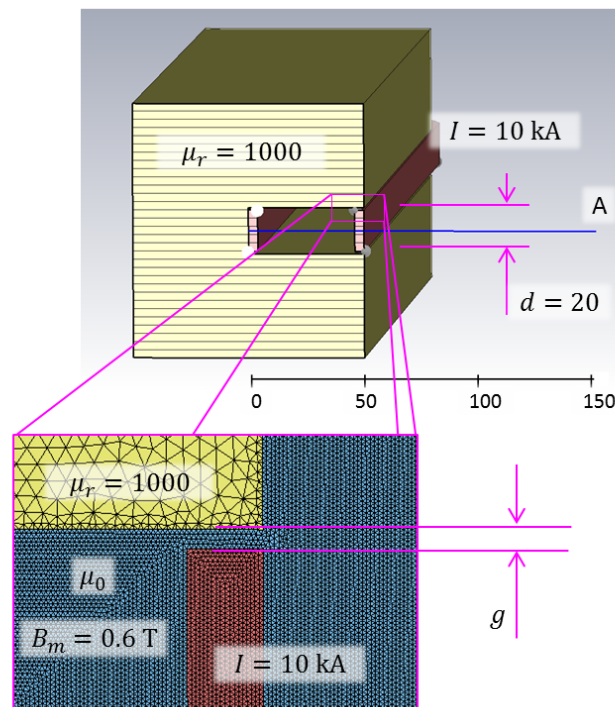


Fig. 12: Simplified static model of the magnet and evaluation of the leakage field as a function of the gap between the septum conductor and the magnetic core.

We will use a set of example parameters to illustrate some of the practical difficulties that arise in the septum magnet design process. For simplicity, these will be used for several different types of septa and that is why the values are not necessarily practical (acceptable) for all discussed septa types.

Example parameters:*

- Gap height: 20 mm
- Gap width: 40 mm
- Relative permeability of the magnetic core: 1000
- Septum thickness: 4 mm
- Septum current: 10 kA
- Septum field: 0.6 T.

*Caution! The chosen parameters are **only** for illustrative purposes and may **not** be practical for all discussed septa types.

Figure 13 shows the normalized absolute value of the magnetic flux density along line A. The main field homogeneity does not change significantly with a change in the gap g but the leakage field is strongly affected. The leakage field is relatively large ($\sim 0.5\%$ of the main field) even when the gap g is zero. Additional measures could be necessary (magnetic screening, more complex septum shape) to bring the leakage field within acceptable limits.

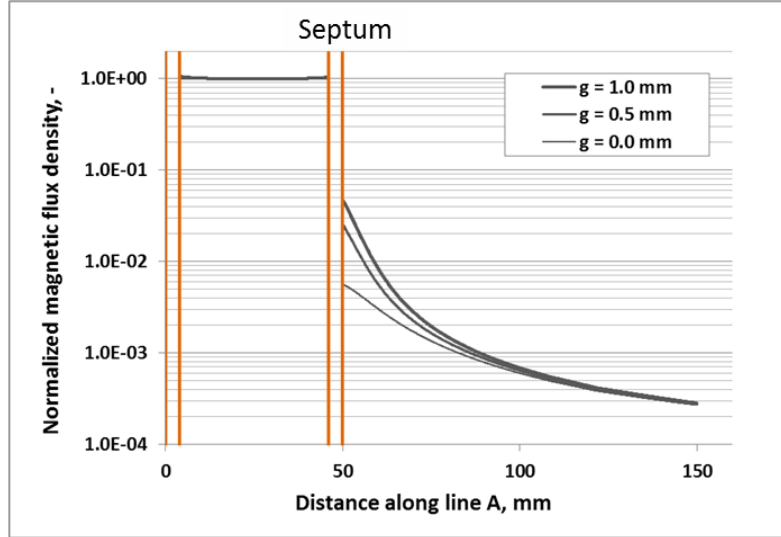


Fig. 13: Normalized absolute value of magnetic flux density along line A

For the given example:

- Septum current density: 125 A/mm^2
- Dissipated power in the septum conductor: 21 kW/m .

Keeping the septum conductor thin results in a reduced cross-section and increases its current density J expressed in A/mm^2 (Eq. (12)):

$$J = \frac{I}{A_s}, \quad (12)$$

where I is the septum current and A_s is the septum cross-section (in mm^2). Due to the high current density, direct drive DC septa have a significant thermal loading. The dissipated power of a copper septum per metre P_{Cu} is given below:

$$P_{\text{Cu}} \approx 1.68 \times 10^{-2} \frac{I^2}{A_s}. \quad (13)$$

Resistance of metallic conductors depends on their temperature. Equation (14) gives the dependency of the resistance R for non-cryogenic temperatures.

$$R = R_0 [1 + \alpha(T - T_0)], \quad (14)$$

where R_0 is the initial resistance, α is the dimensionless coefficient, which depends on the particular conductor metal, T_0 is the initial conductor temperature, and T is the actual conductor temperature. Since the resistance is proportional to the conductor temperature, in constant current systems a thermal runaway could occur.

Note:

- Copper wire operating 50°C above its initial temperature has 20% more resistance.

To avoid overheating, adequate cooling should be provided. Often a fluid is pumped through channels in the conductor to remove the generated heat. Equation (15) gives the removed power P_r as a function of the cooling fluid parameters.

$$P_r = \dot{m}c_p(T_{\text{Out}} - T_{\text{In}}), \quad (15)$$

where \dot{m} is the fluid mass flow rate, c_p is the specific heat capacity of the cooling fluid, T_{Out} is the fluid output temperature, and T_{In} is the fluid input temperature. Depending on its speed, the fluid flow could be laminar or turbulent. Turbulent flow removes heat much more efficiently but too high of a flow rate could cause vibrations and erosion. The Reynolds number R_e characterizes the fluid flow. If $R_e < 2000$ the flow is laminar and if $R_e > 4000$ the flow is turbulent.

$$R_e = \frac{\rho v D}{\mu}, \quad (16)$$

where ρ is the fluid density, v is the mean fluid velocity, D is the internal pipe diameter, and μ is the fluid dynamic viscosity. Another important parameter of the cooling system is the pressure drop over the cooled element and connecting pipes. Equation (17) gives the pressure drop Δp over a pipe with internal diameter D and Darcy friction factor f_D :

$$\Delta p = f_D \frac{\rho v^2}{2D}. \quad (17)$$

Septa should be properly supported to withstand the electromagnetic force generated by the flowing electrical current. Equation (18) gives the electromagnetic force per metre of the septum.

$$F = \frac{BI}{2}, \quad (18)$$

where B is the magnetic flux density and I is the septum current.

For the given example:

- Required cooling water flow rate ('in' to 'out' temperature difference 40°C) per metre is 0.13 kg/s.m or 7.5 l/min.m
- For 4 cooling channels with diameter 3 mm and surface roughness 10 μm , the Reynolds number is 28 500 (definitively turbulent flow)
- Water pressure drop per metre is 1 bar
- The septum will be pushed out of the magnet's gap with a force per metre as high as 3 kN/m or 320 kg/m.

Insulation of the conductors in septa is another important factor for reliable operation. Septa are often the places with the highest radiation levels across the entire accelerator. Organic insulating materials (in the magnet and in its proximity) are vulnerable to high levels of radiation. Radiation resistant insulating materials should be used wherever possible (see Ref. [19]). Depending on the radiation levels, vulnerable components (insulating oil, nearby cables) should be exchanged in a timely manner to avoid failures.

An example of direct drive DC septum 'ISEP2' in the rapid cycling synchrotron (RCS) ring at the Japan Proton Accelerator Research Complex (J-PARC) is shown in Fig. 14. Table 7 gives its basic design parameters (see Refs. [20–22]).

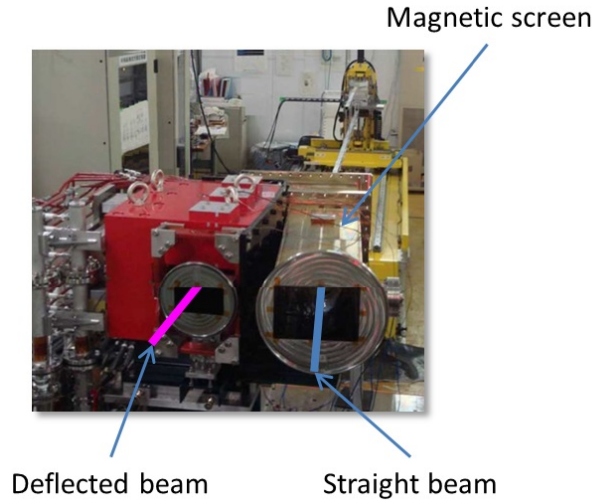


Fig. 14: Direct drive DC septum ISEP2 in RCS ring (J-PARC)

Table 7: Specification of direct drive DC septum ISEP2 in RCS ring (J-PARC)

Parameter	Value
Device design	“In-air”
Field length, mm	650
Gap height, mm	140
Gap width, mm	348
Beam momentum, MeV/c	181
Deflection angle, mrad	90.8
Septum thickness, mm	45
Current, kA	6
Magnetic flux density, T	0.475

5.2 Direct drive low frequency (LF) pulsed septum

The direct drive LF pulsed septum is very similar to the direct drive DC septum, excepting that the current does not flow all the time but it is pulsed. Pulsed operation reduces the overall consumption of the device and reduces the stored *beam* disturbance in circular accelerators. Moreover, it reduces the average dissipation in the septum and makes it possible to increase the septum current, and to operate at higher magnetic fields with reduced septum thickness. The ratio of the time period t when the septum is powered and the repetition rate period T is called the duty cycle δ :

$$\delta = \frac{t}{T}. \quad (19)$$

The root-mean-square current of a rectangular pulse is $\sqrt{\frac{1}{\delta}}$ times smaller than the maximum pulse current. For a half-sine pulse this coefficient is $\sqrt{\frac{2}{\delta}}$. Short pulses deposit the heat virtually instantaneously, creating large thermal cycling (see Ref. [23]).

Large currents produce large electromagnetic forces and if they are pulsed, strong dynamic mechanical stresses (known as ‘hammering’) are generated. Adequate mechanical support is needed to prevent septum displacement. If not properly designed, constantly vibrating conductors could ‘cut

through' their isolating supports, leading to catastrophic failure. Some designs include dedicated shock absorbers to limit the mechanical wave transfer to the rest of the device.

Note:

- For short pulses there is no effective heat transfer and the case should be treated as if the pulses deposit the heat instantaneously.
- For a septum operating at 1 T with a 30 kA pulse, the maximum force per metre could be as large as 15 kN/m or 1500 kg/m.

A step-down transformer can be used to provide the required high current. Typically the transformation ratio is in the range 4:1 to 50:1. In septa having a sine-wave current pulse, a third harmonic circuit can be used to improve the flat top of the pulse. The fundamental and third harmonic current add together to widen the flat top. In some amplitude-sensitive applications, an active electrical regulation circuit may improve further the stability of the flat-top current (see Ref. [3]).

Figure 15 shows a typical example of an 'in-vacuum' direct drive LF pulsed septum PESMH16 used in the proton synchrotron (PS) at CERN. Its basic parameters are listed in Table 8 (see Refs. [24, 25]).

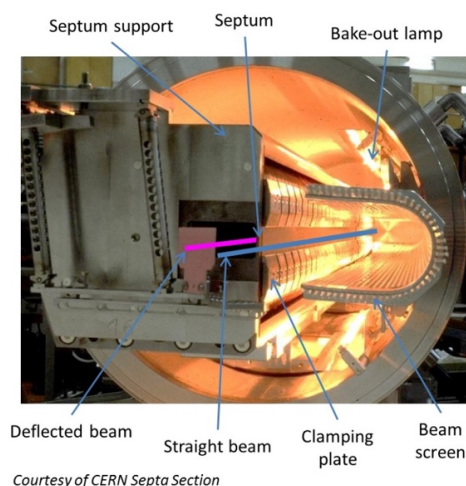


Fig. 15: Direct drive LF pulsed septum PESMH16 (PS, CERN)

Table 8: Specification of direct drive LF pulsed septum PESMH16 (PS, CERN)

Parameter	Value
Device design	'In-vacuum'
Vacuum, mbar	10^{-9}
Field length, mm	2180
Gap height, mm	30
Gap width, mm	65
Beam momentum, GeV/c	25.1
Deflection angle, mrad	30
Septum thickness, mm	3
Current, kA	28.5 (half-sine 3.5 ms)
Magnetic flux density, T	1.2

5.3 In-air Lambertson septum

Due to magnetic circuit symmetry, the zero-field region of the Lambertson septum has a very low leakage field and disturbs very little the stored *beam* in circular accelerators. This design allows for a thin septum. The device could be DC or LF pulsed. Lambertson septa have a more complex geometry and deflect the *beam perpendicular to the initial displacement*. Figure 16 shows a typical example of an ‘in-air’ DC Lambertson septum MSIA in the large hadron collider (LHC) at CERN (see Refs. [26,27]) and Table 9 summarizes its basic parameters. This particular design is characterized by two zero-field channels (for circulating *beam* and for counter rotating *beam*). Mu metal chambers are used for additional magnetic screening. A non-evaporable getter (NEG) coating is deposited on the inner surface of the chamber to improve the local vacuum. The top yoke side (with zero-field channels) extends 175 mm on each side of the device to screen the fringe magnetic fields.

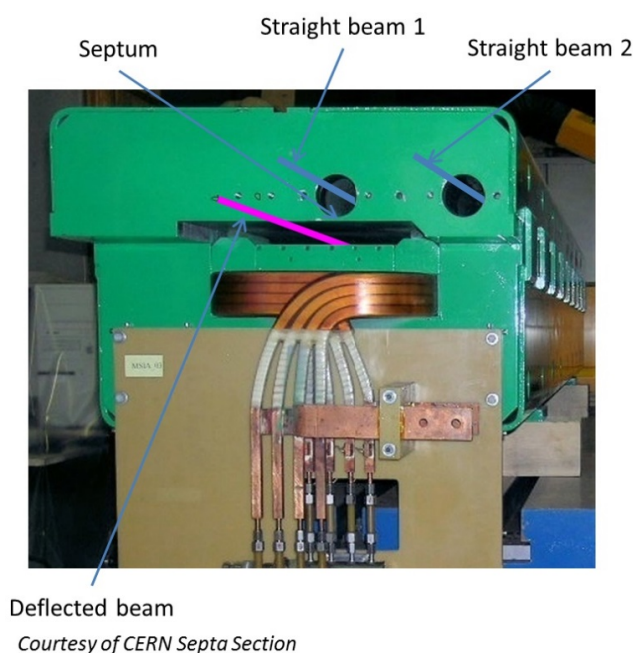


Fig. 16: Lambertson DC septum MSIA in LHC at CERN

Table 9: Specification of Lambertson DC septum MSIA (LHC, CERN)

Parameter	Value
Device design	‘In-air’
Vacuum, mbar	10^{-7}
Field length, mm	3650
Gap height, mm	25
Gap width, mm	230
<i>Beam</i> momentum, GeV/c	450
Deflection angle, mrad	1.846
Septum thickness, mm	6
Current, kA	0.95×16 turns
Magnetic flux density, T	0.76

5.4 Half in-vacuum Lambertson septum

Another example of a DC Lambertson septum is the ‘half-in-vacuum’ septum for SwissFEL at the Paul Scherrer Institute (PSI). It benefits from a relative low vacuum volume and a very thin septum wall. The coil is on the air side, which makes it easily serviceable. The massive additional shorted electrical turn reduces HF current ripples from the power supply. The bottom yoke side (with zero-field channel) extends 150 mm on each side to screen the fringe magnetic fields. Figure 17 shows the ‘half-in-vacuum’ DC Lambertson septum AFS for SwissFEL switchyard and Table 10 summarizes its basic parameters (see Ref. [28]).

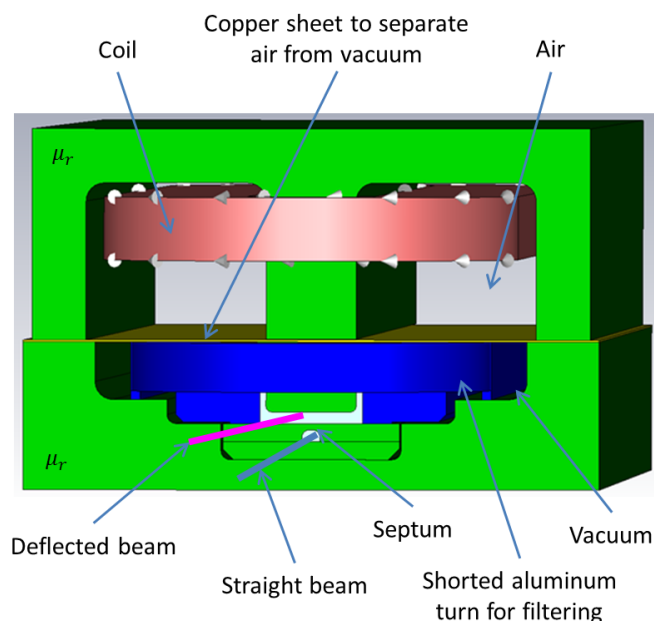


Fig. 17: Lambertson DC septum MSIA in LHC at CERN

Table 10: Specification of Lambertson DC septum MSIA (LHC, CERN)

Parameter	Value
Device design	‘Half-in-vacuum’
Vacuum, mbar	10^{-7}
Field length, mm	760
Gap height, mm	6.8
Gap width, mm	61
Beam momentum, GeV/c	3.15
Deflection angle, mrad	35
Septum thickness, mm	2.5
Current, kA	0.1×41 turns
Magnetic flux density, T	0.51

5.5 Opposite field septum

Instead of a zero-field region the opposite field septa have a region with a magnetic field in the opposite direction (see Ref. [29]). In this way the electromagnetic forces at the septum cancel out and the mechanical aspects of septum support are relaxed. Both *beams* are deflected but in the opposite direction. The design could be DC or LF pulsed. An example of an opposite field ‘in-air’ design, LF

pulsed septum is the injection septum (Fig. 18) used at the Japan Proton Accelerator Research Complex (J-PARC) at The High Energy Accelerator Research Organization known as KEK. Table 11 gives its basic parameters (see Ref. [30]).

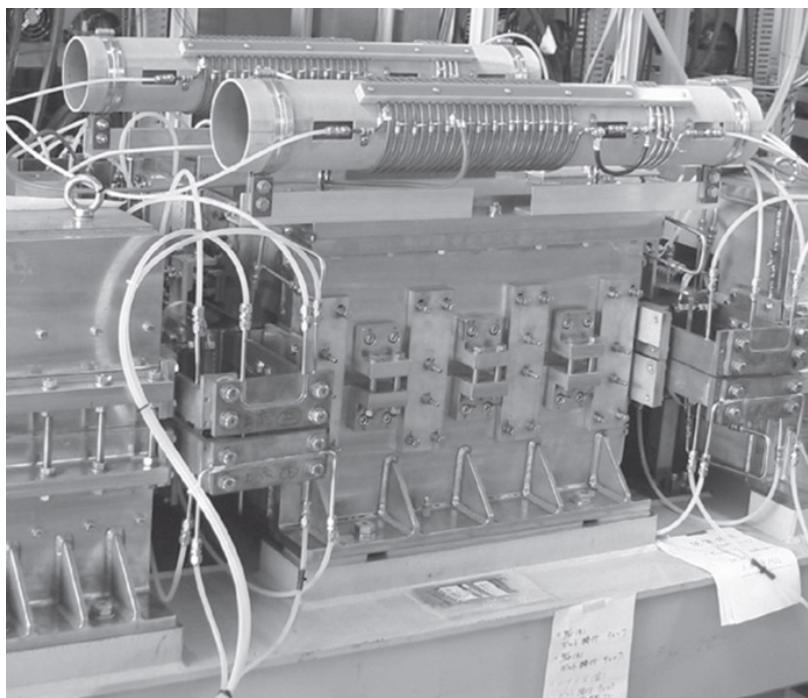


Fig. 18: Opposite field septum at J-PARK (KEK)

Table 11: Specification of opposite field LF pulsed septum at J-PARK (KEK)

Parameter	Value
Device design	'In-air'
Field length, mm	700
Gap height, mm	120
Gap width, mm	150/400
Beam momentum, GeV/c	3
Deflection angle, mrad	68
Septum thickness, mm	8
Current, kA	48 × 2 (half-sine 2.5 ms)
Magnetic flux density, T	0.6

5.6 Massless septum

A 'massless septum' idea is to create two distinctive magnetic field regions without using a physical barrier (physical septum) between them. A complex magnetic circuit and/or several excitation coils have to create the two field regions (Refs. [31,32]). An illustration of this approach is given by the design proposed at the Nuclear Science Research Facility (NSRF) at Kyoto University (Ref. [32]). The design can be DC or pulsed. The absence of a physical septum means there is no interaction with the *beam* and no *beam* losses and no radiation. The drawback of the design is the gradual transition between the two field regions, making the effective septum very thick. If the *beam* crosses through this transition region (with a field gradient) the accelerator optics can be compromised. As a 'rule of thumb' the gradient region is approximately the same as the magnetic gap height (or the distance between the closest current

conductors). A cross-section of a static magnetic simulation model and the field profile along line A is shown in Fig. 19.

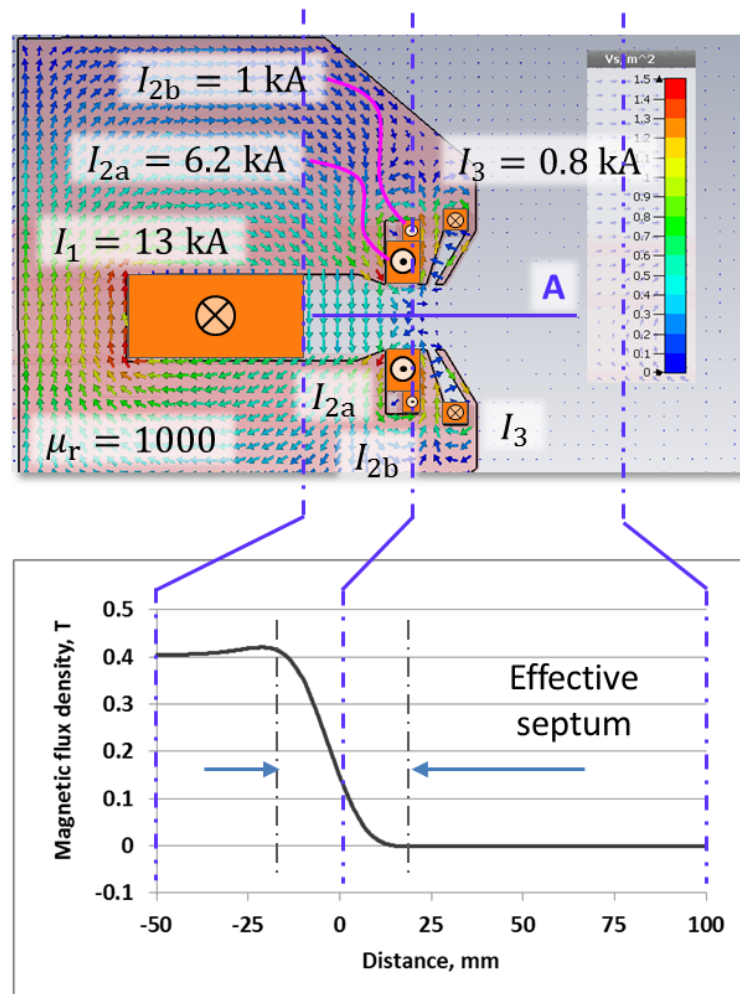


Fig. 19: Static magnetic simulation model of the proposed massless septum design and magnetic field profile along line A.

5.7 Eddy current septum

If the magnetic field changes inside of a solid conductor, (eddy) currents will be induced to oppose the magnetic field change. This effect is utilized to design very thin septa devices. The magnetic field in the field region is established relatively quickly and due to the eddy currents in the septum conductor the field does not penetrate through it. The septum acts as very efficient screen, keeping the magnetic field in the zero-field region at a very low level. Due to the fact that the eddy currents are produced by changing magnetic fields only, this scheme does not work for DC magnets. The designer of an eddy current septum needs to find a good engineering compromise between the thickness of the septum and the rate of change of the magnetic field. The higher the magnetic field change rate is, the thinner septum that is needed. Due to the dynamic behaviour of the eddy currents they attenuate well the high frequency components of the magnetic pulses but they screen poorly the low frequency ones. The low frequency pulse components, even though attenuated, propagate slowly through the septum and they appear on the other side with a large time delay. This delay could be several times longer than the magnetic pulse itself and could be easily overlooked in time domain simulations. Especially in circular accelerators, this

delayed leakage field could compromise the overall performance of the septum. Some additional magnetic screening could further improve the leakage field performance.

Eddy current septa use short (high frequency) current pulses and they are classified in a different group to emphasize the importance of the current pulse time profile for their proper operation. The need for a large magnetic field change rate requires a low magnet inductance and adds complexity to their pulsed power supplies. Usually, this type of magnet has one turn excitation coil to maintain the magnet's inductance and the required operating voltage low. Demanding electrical switches are needed to produce the short and large amplitude current pulses. Nevertheless, eddy current septa provide the thinnest magnetic septum and very good magnetic field screening, reaching main field to leakage field ratios of over 1000:1.

In the literature (see Refs. [33–35]) it is possible to find analytical models that describe the delayed propagation of the leakage field through a septum. Figure 20 illustrates its behaviour for a 5 mm thick copper septum, 1 T square main pulse field with duration 20 μ s.

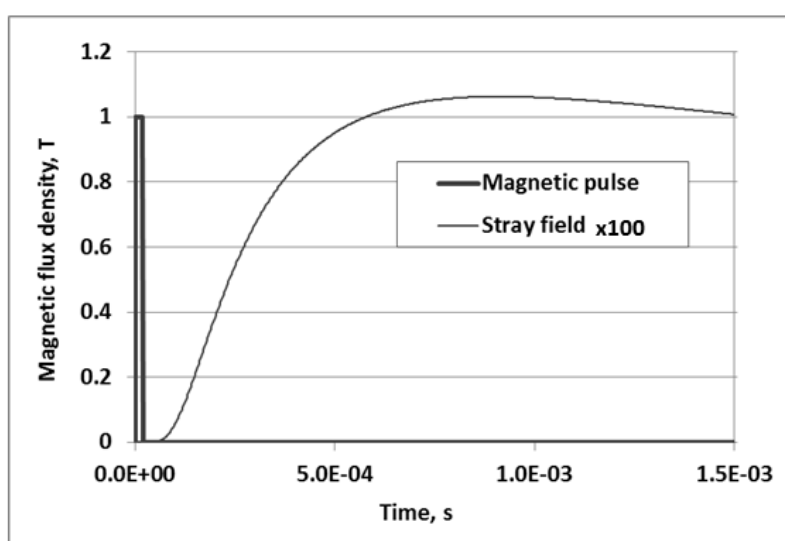


Fig. 20: Delayed leakage field from short unipolar magnetic pulse

Equations (20) and (21) describe analytically the delay time t_m at which the leakage field reaches its maximum value B_m (Ref. [34]):

$$t_m = \frac{1}{2} d_s^2 \sigma \mu, \quad (20)$$

$$B_m = B_0 \frac{2\sqrt{2}\tau}{d_s \sigma \mu \lambda_c \sqrt{\pi \epsilon}}, \quad (21)$$

where d_s is the septum thickness, σ is the septum conductivity, μ is the septum permeability, B_0 is the amplitude of the main field, τ is the width of the pulse, and λ_c is the characteristic length of stray field decay.

In order to find an analytical solution, sometimes these methods simplify the problem using approximations and assumptions that deteriorate the result accuracy. They are often good for a qualitative understanding of the problem but show quantitative discrepancies with the real results. Other methods, such as 3D electromagnetic simulation or direct measurements, should be considered to gain confidence in the result.

The presence of a DC (or low frequency) component in the main field affects strongly the screening performance of eddy current septa. Figure 21 shows the measured leakage field (upper graph)

for different main field pulse waveforms (lower graph). Pulses with zero DC component yield the lowest leakage field.

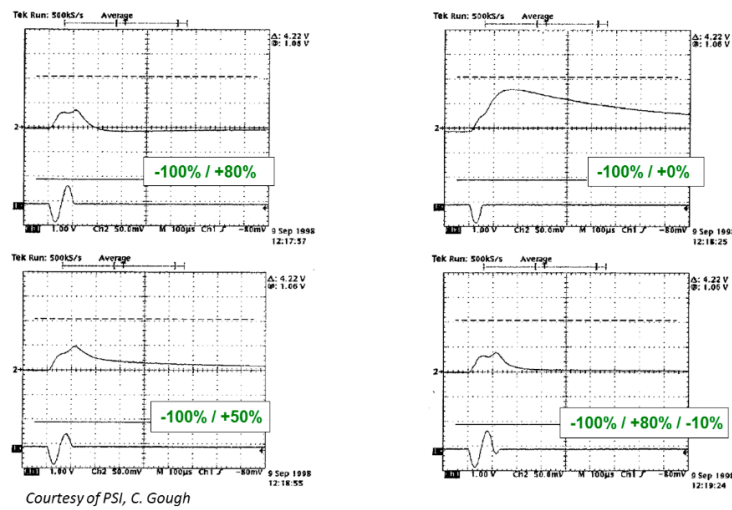


Fig. 21: Eddy current screening performance for different pulse shapes

A typical example of an eddy current septum is the ‘in-vacuum’ injection septum Y12 of the Swiss light source (SLS) at the Paul Scherer Institute (PSI), shown in Fig. 22 (Ref. [36]). Table 12 summarizes its basic parameters.

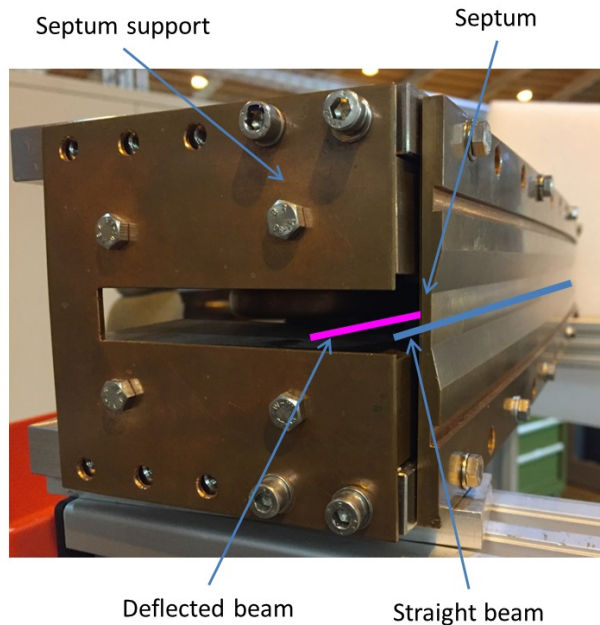


Fig. 22: ‘In-vacuum’ injection septum Y12 (SLS, PSI)

In this particular design, the eddy current septum reduces the leakage field to less than 0.1% of the main field. After adding an additional magnetic screening around the circulating beam (pipe of thin μm metal sheet) the leakage field is practically ‘invisible’ to the used measurement method ($< 10^{-5}$ of the main field) – see Refs. [36,37].

Table 12: Specification of ‘In-vacuum’ injection septum Y12 (SLS, PSI)

Parameter	Value
Device design	‘In-vacuum’
Vacuum, mbar	10^{-7}
Field length, mm	600
Gap height, mm	6
Gap width, mm	20
Beam momentum, GeV/c	2.4
Deflection angle, mrad	70
Septum thickness, mm	2.5
Current, kA	4.3 (full-sine 0.16 ms)
Magnetic flux density, T	0.9

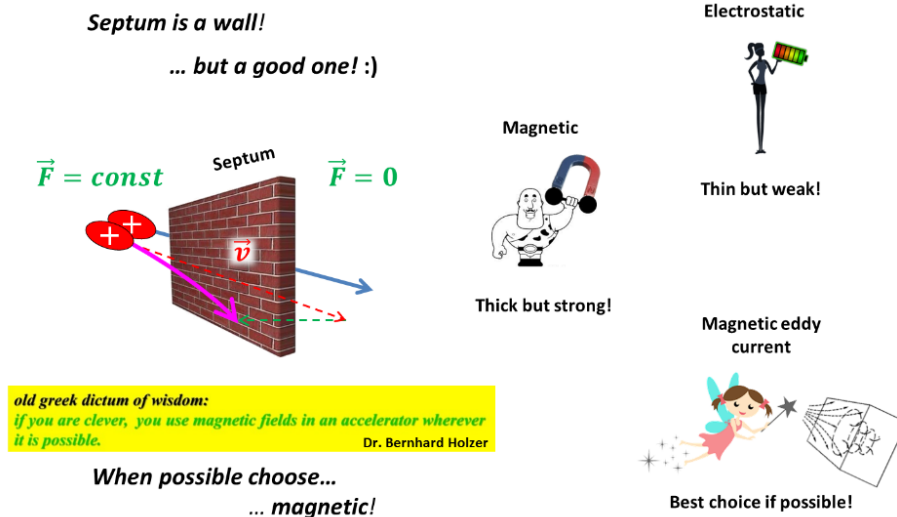
5.8 Practical considerations

- (i) *High mechanical and thermal stress* – Adequate septum support should be used in order to handle the electromagnetic forces. Mechanical damping can reduce the effect of ‘hammering’. Attention should be given to coping with large thermal cycling and adequate cooling should be provided.
- (ii) *The maximum leakage field of eddy current septum is delayed* – An eddy current septum should be thick enough to effectively screen the main field. Attention should be given to the fact that some leakage field could appear on the other side of the septum (penetrate the septum) with a long delay. Additional screening might be needed to deal with the problem.
- (iii) *Good field region* – Field homogeneity could be improved using magnetic poles geometry (shims etc.).
- (iv) *Leakage dipole field* – Additional magnetic shielding might improve septum performance. Care should be taken that the shielding material does not saturate.
- (v) *Beam impedance* – Beam impedance changes should be minimized using proper screening.
- (vi) *Cooling* – Turbulent flow removes heat more efficiently but it increases the erosion rate and vibrations.
- (vii) *Insulators degradation* – Use radiation-hard isolation materials whenever possible. In high radiation level areas, vulnerable materials (cable insulation, insulation oil) have to be exchanged in a timely manner to avoid failures.
- (viii) *Alignment* – Use adequate (remote) positioning systems.
- (ix) *Good vacuum* – Good vacuum septa should be bake-out compatible. Initial investment in integrating in situ bake-out systems could save long term costs and effort especially if the vacuum is often broken. Good vacuum conductivity and NEG coatings should be combined to maintain low background gas pressure.
- (x) *Machine protection* – Septa are often the highest energy density elements within the entire accelerator. Adequate machine protection should be used to avoid damage in case of system failure or operator error.
- (xi) *Avoid brazed joints in vacuum as much as possible* – Brazed joints are often the most likely places for a failure to occur.
- (xii) *Vacuum (cold) welding* – In the absence of air or other contaminants, metal surfaces (of the same metal) in contact could undergo ‘cold welding’, fusing permanently the two elements into one piece of metal. Use silver-plated bolts in steel threads to avoid bolts jamming.

- (xiii) *Activation* – Care should be taken when handling activated materials. Maintenance should be done according to the radiation safety regulations.

(This list is not exhaustive.)

5.9 What to remember



Acknowledgements

Special thanks go to Dr Mike Barnes (CERN) for providing very useful material, Chris Gough (PSI) for providing very useful material and Dr Sladana Dordevic (PSI) for helping with the field simulations.

References

- [1] A. Afonin, *et al.*, Proton Extraction from IHEP Accelerator Using Bent Crystals, International Workshop on Relativistic. Channeling and Related Coherent Phenomena, Italy, 2004.
- [2] S. Baker *et al.*, *Nucl. Instrum. Methods* **A234** (1985), 602, [https://doi.org/10.1016/0168-9002\(85\)91014-9](https://doi.org/10.1016/0168-9002(85)91014-9).
- [3] M. Barnes, Beam Transfer Devices Septa, CAS-CERN Accelerator School, Belgium, 2009.
- [4] C. Bovet *et al.*, A selection of formulae and data useful for the design of A.G. synchrotrons (CERN, Switzerland, 1970).
- [5] B. Holzer, Introduction to transverse beam dynamics, CAS-CERN Accelerator School, Slovakia, 2012.
- [6] K. Wille, *The Physics of Particle Accelerators: An Introduction* (Oxford University Press, Oxford, 2000), p. 148.
- [7] M. Reiser, *Theory and Design of Charged Particle Beams* (Wiley, New Jersey, 2008), p. 18.
- [8] J. Borburgh *et al.*, Final results on the CERN PS electrostatic septa consolidation program (PAC, USA, 2003).
- [9] J. Borburgh *et al.*, Consolidation project of the electrostatic septa in the CERN PS ring (PAC, USA, 2001).

- [10] L. Sermeus *et al.*, The Design of the special magnets for PIMMS/TERA (EPAC, Switzerland, 2004).
- [11] P. Bryant *et al.*, Proton-Ion Medical Machine Study (PIMMS) Part II, CERN-PS-2000-007-DR (CERN, Switzerland, 2000).
- [12] J. Borburgh *et al.*, Design and construction of the LEIR injection septa, LHC Project Report 810 (CERN, 2005).
- [13] J. Wenninger, Introduction to slow extraction to the North Targets, Training for operation (CERN, Switzerland, 2007).
- [14] R. Barlow *et al.*, A new spark detection system for the electrostatic septa of the SPS North Targets, 14th ICALEPCS, USA, 2013.
- [15] B. Goddard *et al.*, Beam loss damage in wire septum, EPAC 2000, Austria, 2000.
- [16] H. Schonauer, Loss management studies for the PSB, Summary of the CERN Meeting on Absorbers and Collimators for the LHC, CERN, 2002.
- [17] H. Schonauer, Loss concentration and evacuation by mini-wire-septa from circular machines for spallation neutron sources (PAC, USA, 1995).
- [18] M. Traveria, *Nucl. Instrum. Methods* **A412** (1998), 183, [https://doi.org/10.1016/S0168-9002\(98\)00582-8](https://doi.org/10.1016/S0168-9002(98)00582-8).
- [19] A. Gabard *et al.*, Radiation hard magnets at the Paul Scherrer Institute, IPAC, USA, 2012, pp. 3518–3520.
- [20] M. Yoshimoto *et al.*, Designs of Septum Magnet at 3 GeV RCS in J-PARC, EPAC, Scotland, 2006.
- [21] M. Watanabe *et al.*, *IEEE Trans. Appl. Supercond.* **16** (2006).
- [22] M. Yoshimoto *et al.*, *IEEE Trans. Appl. Supercond.* **18** (2008).
- [23] K. Fan *et al.*, *Nucl. Instrum. Methods* **A565** (2006), 439, <https://doi.org/10.1016/j.nima.2006.06.031>.
- [24] J. Borburgh *et al.*, A new set of magnetic septa in the CERN PS Complex (PAC, USA, 1999).
- [25] D. Manglunki *et al.*, Beam extraction, PS/SPS User Meeting 2015, CERN, Switzerland, 2015.
- [26] O. Bruning *et al.*, LHC Design Report, Vol.1 The LHC Main Ring, Ch. 16 Injection System, (CERN, Geneva, 2004).
- [27] M. Gyr, Expected magnetic field quality of the LHC septum magnets used for injection (MSI) and for extraction to the beam dump (MSD), LHC Project Note 129/rev. (CERN, Switzerland, 1999).
- [28] S. Dordevic, SwssFEL Septum, Internal presentation, 2016.
- [29] I. Sakai *et al.*, Operation of an opposite-field septum magnet for the J-Parc main-ring injection (EPAC, Scotland, 2006).
- [30] K. Fan, *Nucl. Instrum. Methods* **A597** (2008), 142.
- [31] S. Fartoukh, A semi-analytical method to generate an arbitrary 2D magnetic field and determine the associated current distribution, LHC Project Report 1012 (CERN, Switzerland, 2007).
- [32] Y. Iwashita *et al.*, Massless septum with hybrid magnet (PAC, Sweden, 1998).
- [33] W. Kang *et al.*, Development of an eddy-current septum magnet for the SSRF storage ring (APAC, China, 2001).
- [34] W. Kang *et al.*, Study on the Stray field of the eddy-current septum magnet for the SSRF storage ring China.
- [35] B. Kang *et al.*, *Nucl. Instrum. Methods* **385** (1997), 6, [https://doi.org/10.1016/S0168-9002\(96\)01025-X](https://doi.org/10.1016/S0168-9002(96)01025-X).

- [36] C. Gough, Minimizing leakage field from eddy current septum magnets, Presentation at SINAP 2005.
- [37] C. Gough *et al.*, Septum and kicker systems for the SLS (PAC, USA, 2001), <https://doi.org/10.1109/PAC.2001.988238>.

Appendix A: Derivation of electrostatic deflection equation

All quantities are in SI units unless otherwise stated.

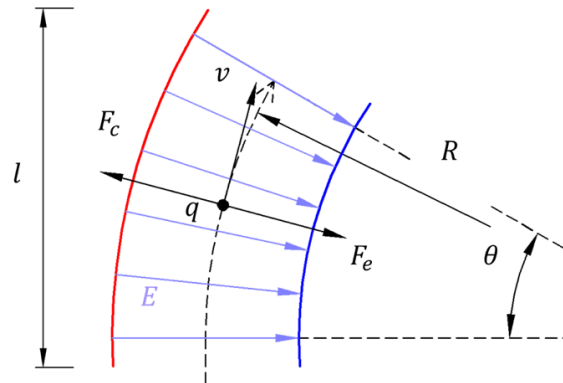


Fig. A.1: Charged particle travelling between curved electrodes that follow the particle's trajectory

Charged particle q with elementary charge q_e (positive) travels with instantaneous velocity v between curved electrodes that follow the particle's trajectory (as shown in Fig. A.1, where the red line represents positive and blue the negative electrode) and they create a constant electric field E along the particle's trajectory. The field is always perpendicular to the direction the particles travel, and the particle will experience a constant electric force F_e , always perpendicular to the particles direction of travel, and it will follow an arc trajectory with radius R , balancing the electric field force F_e and the centrifugal force F_c . Equations (A.1) and (A.2) express the electric force and the centrifugal force respectively.

$$F_e = q_e E, \quad (\text{A.1})$$

$$F_c = \frac{\gamma m_0 v^2}{R}, \quad (\text{A.2})$$

where γ is a relativistic factor that takes into account the transverse relativistic effects on the particle dynamics with rest mass m_0 . If the particle does not experience other forces the electric force F_e is equal and opposite to the centrifugal force F_c :

$$q_e E = \frac{\gamma m_0 v^2}{R}. \quad (\text{A.3})$$

Expressing the arc trajectory radius R we have

$$R = \frac{\gamma m_0 v^2}{q_e E}, \quad (\text{A.4})$$

$$p = \gamma m_0 \beta c, \quad (\text{A.5})$$

$$v = \beta c. \quad (\text{A.6})$$

Substituting the relativistic factor γ , using relativistic momentum p (Eq. (A.5)) and the velocity of the particle v expressed by the relativistic factor β (Eq. (A.6)) for the arc trajectory radius R we have

$$R = \frac{p\beta c}{q_e E}. \quad (\text{A.7})$$

Changing the particle's momentum from SI units $[\frac{\text{kg}\cdot\text{m}}{\text{s}}]$ to accelerator units $[\frac{\text{GeV}}{c}]$, using Eq. (A.8) yields

$$p[\frac{\text{kg}\cdot\text{m}}{\text{s}}] = \frac{10^9 q_e}{c} p[\frac{\text{GeV}}{c}], \quad (\text{A.8})$$

$$R = \frac{10^9 \beta p}{E}. \quad (\text{A.9})$$

For a bending radius R much larger than the length of the deflecting field l we can express the bending angle θ using the small angle approximation $\tan(\theta) \approx \theta$:

$$\theta \approx \frac{l}{R}. \quad (\text{A.10})$$

Substituting R in Eq. (31) we obtain the final expression for the bending angle θ (note the momentum p is in GeV/c)

$$\theta \approx \frac{El}{10^9 \beta p}. \quad (\text{A.11})$$

Geometrical length of a septum differs from the electric field length due to the mechanical construction and/or the fringe fields and an integral effective value l_{eff} is used to describe more precisely the effective interaction length.

To emphasize the parallel between (the duality of) the electric and magnetic deflection, curved electrodes are used to produce the deflecting electric field, always perpendicular to the particle's direction of travel. As we will see later, this is the case for magnetic deflection.

In practice, straight deflecting electrodes are more often used. It can be shown that if the deflection angle is small (gained transverse velocity v_x is much smaller than main velocity v_z), Eq. (A.11) gives still a good approximation of the deflection even for straight electrodes.

Appendix B: Derivation of magnetic deflection equation

All quantities are in SI units unless otherwise stated.

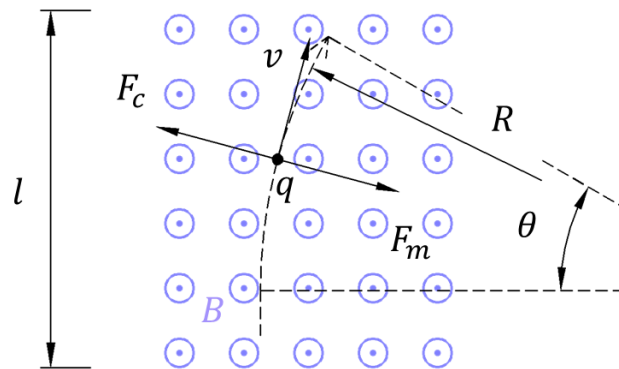


Fig. B.1: Charged particle travelling in transverse magnetic field

Charged particle q with elementary charge q_e (positive) travels with instantaneous velocity v through a constant transverse magnetic field B , going out of the plane of the paper (as shown in Fig. B.1). The particle will experience a constant magnetic force F_m , always perpendicular to the particles direction of travel and to the direction of the magnetic field, and it will follow an arc trajectory with radius R , balancing the magnetic field force F_m and the centrifugal force F_c . Equations (B.1) and (B.2) express the scalar form of the magnetic force and the centrifugal force respectively.

$$F_m = q_e v B , \quad (\text{B.1})$$

$$F_c = \frac{\gamma m_0 v^2}{R} , \quad (\text{B.2})$$

where γ is a relativistic factor to take into account the transverse relativistic effects on particle's the dynamics with rest mass m_0 . If the particle does not experience other forces the magnetic force F_m is equal and opposite to the centrifugal force F_c :

$$q_e v B = \frac{\gamma m_0 v^2}{R} . \quad (\text{B.3})$$

Expressing the arc trajectory radius R we have

$$R = \frac{\gamma m_0 v^2}{q_e v B} , \quad (\text{B.4})$$

$$p = \gamma m_0 \beta c , \quad (\text{B.5})$$

$$v = \beta c . \quad (\text{B.6})$$

Substituting the relativistic factor γ , using the relativistic momentum p (Eq. (B.5)) and the velocity of the particle v expressed by the relativistic factor β (Eq. (B.6)) for the arc trajectory radius R we have

$$R = \frac{p}{q_e B} . \quad (\text{B.7})$$

Changing the particle's momentum from SI units $[\frac{\text{kg}\cdot\text{m}}{\text{s}}]$ to accelerator units $[\frac{\text{GeV}}{c}]$ using Eq. (B.8) and using the approximate value of the speed of light $c \approx 3 \times 10^8$ m/s, yields

$$p[\frac{\text{kg}\cdot\text{m}}{\text{s}}] = \frac{10^9 q_e}{c} p[\frac{\text{GeV}}{c}] , \quad (\text{B.8})$$

$$R \approx \frac{10^9 p}{3 \times 10^8 B} \approx \frac{p}{0.3 B} . \quad (\text{B.9})$$

For a bending radius R much larger than the length of the deflecting field l we can express the bending angle θ using the small angle approximation $\tan(\theta) \approx \theta$:

$$\theta \approx \frac{l}{R} . \quad (\text{B.10})$$

Substituting R in Eq. (B.10) we obtain the final expression for the bending angle θ (note the momentum p is in GeV/c)

$$\theta \approx \frac{0.3 B l}{p} . \quad (\text{B.11})$$

Geometrical length of a septum differs from the magnetic field length due to the mechanical construction and/or the fringe fields and an integral effective value l_{eff} is used to describe more precisely the effective interaction length.